Multiple Access using Time Modulated Array with Single RF Chain

Citation for published version:
He, X, Ding, Y & Huang, G 2019, 'Multiple Access using Time Modulated Array with Single RF Chain', *Recent Advances in Electrical and Electronic Engineering*, vol. 12, no. 5, pp. 395-401.
https://doi.org/10.2174/2352096511666180705120210

Digital Object Identifier (DOI):
10.2174/2352096511666180705120210

Link:
Link to publication record in Heriot-Watt Research Portal

Document Version:
Peer reviewed version

Published In:
Recent Advances in Electrical and Electronic Engineering

Multiple Access using Time Modulated Array with Single RF Chain

Xu He[a], Yuan Ding[*b] and Gaojian Huang[c]

[a]*The School of Communications and Information Engineering, Xi'an University of Posts and Telecommunications, Xi'an, China, 710121;*

[b] *The Institute of Sensors, Signals and Systems (ISSS), Heriot-Watt University, United Kingdom, EH14 4AS;*

[c] *The Institute of Information and Communications, Guilin University of Electronic Technology, Guilin, China, 541004*

Abstract: A new wireless multiple access technology enabled by using time modulated arrays (TMAs) is proposed in this paper. It benefits from the requirement of only a single radio frequency (RF) chain, compared with other multiple-RF-chain schemes. As a result, it is able to greatly reduce the system cost, energy consumption, and complexity. In addition, the signal through the single RF chain is narrow-band modulated, reducing the signal peak-to-average-power ratio (PAPR), thus, further enhancing the power efficiency of the RF chain, especially for power amplifiers. The operation principle and synthesis approach are elaborated in this paper, and are demonstrated with two examples.

Keywords: Fourier series, multiple access, radio frequency (RF) chains, space-division multiple access (SDMA), time modulated array (TMA), wireless communications.

1. INTRODUCTION

Wireless communications have become increasingly prevalent in our modern society due to their inherent favourable properties, such as scalability, low deployment cost, and applicability to mobile environment. In wireless communication systems, providing data service to multiple users, namely multiple access, is essential. Conventionally, multiple users are served by allocating them orthogonal resources in various domains. Different domains correspond to different multiple access technologies, for examples, time-division multiple access (TDMA) used in GSM systems, frequency-division multiple access (FDMA) used in most satellite communication systems, and code-division multiple access (CDMA) adopted in IS95 and CDMA2000 standards. These multiple access technologies have their advantages and limitations. With respect to limitations, TDMA scheme requires multiple users being precisely synchronised in time and having agreement in time slots assignment, which can impose great overheads and latency when the number of users is huge. While in FDMA schemes, combining multiple data streams at different frequencies results in high signal peak-to-average-power ratio (PAPR), which is, for example, a well-known issue in orthogonal frequency-division multiplexing (OFDM) systems. The high PAPR forces power amplifiers to operate at high output back-off points, leading to extremely low power efficiency. In CDMA systems, the use of spreading codes with a spreading factor *S* reduces the data transmission rates by a factor *S*.

The above three multiple access schemes can operate with a single radio frequency (RF) chain, so that the multiplexed data, in time, frequency, and/or code domains, are broadcasted, which inevitably increase the inter-user interference. Because different users are normally located along different spatial directions, in order to alleviate inter-user interference, the spatial domain can then be exploited. This is known as space-division multiple access (SDMA) [1]. SDMA is commonly used in conjunction with the afore-mentioned three multiple access schemes, and it requires multiple RF chains, exciting an antenna array, with the number no less than the number of users, in order to achieve beamforming gains towards each user. As a consequence, the focused energy to desired users can help alleviate (or even eliminate in some specific conditions) inter-user interference. However, it was pointed out earlier that this requires multiple RF chains, which are the most power hungry and costly components in transmitters.

In this paper, we propose to use time modulated arrays (TMAs), [2], for SDMA in conjunction with FDMA, using only a single RF chain. The proposed TMA multiple access scheme, when compared with other traditional multiple access transmitter architectures, provides a number of benefits, including

---

* The Institute of Sensors, Signals and Systems (ISSS), Heriot-Watt University, United Kingdom, EH14 4AS; Tel: +44(0)1314513029; E-mail: yuan.ding@hw.ac.uk

- No strict time synchronisation is required as it is not based on TDMA;
- No code spreading is used as it is not based on CDMA;
- Although it is based upon FDMA, i.e., different users receive signals at different frequencies, transmitted RF signal PAPR is low, as data for most users are synthesised in RF feeding networks via switches, instead of in digital baseband;
- Only a single RF chain is required at transmitter side;
- Compared with the traditional single RF chain FDMA, the beamforming gain towards different users can be obtained, i.e., SDMA.

This paper is organised as follows: in Section 2, a brief overview of TMAs and their applications are presented. In Section 3, the TMA transmitter architecture used in this paper and associated system assumptions are described. The proposed single RF chain TMA for multiple access purpose is elaborated in Section 4, followed by two examples in Section 5. Finally, the findings in this paper are concluded and further research directions are also identified.

2 OVERVIEWS OF TMA AND ITS APPLICATIONS

Antenna is an important component in wireless communication systems, responsible for converting current to electromagnetic waves, in transmit mode, or vice versa in receive mode. In order to focus energy in a narrow spatial direction, antenna arrays, especially phased array, are commonly adopted. The beamforming property is determined by the array excitation vectors and the array geometry in 3-dimention (3D) space. Thus, they are often referred to as 3D arrays.

By introducing a fourth dimension, time, into the array design, i.e., connecting and disconnecting the array elements from the feeding network in the time domain, the array radiation patterns of the resulting TMAs, also called as 4D arrays, can be controlled [3]. This is made possible because the periodic switching function expands the feeding signals in frequency domain (in Fourier series form). The detailed mathematic expressions will be presented in the next section.

Traditionally, the TMA concept was mainly used for low radiation sidelobe synthesis [4]. This is the direct consequence of spreading energy in frequency domain. Thus, along sidelobe directions at fundamental frequencies the radiated (in transmit mode) or detected (in receive mode) energy at fundamental frequencies is suppressed. More recently, this TMA was found useful in a number of other applications, such as direction finding [5], Radar [6], and physical-layer wireless security [7]. All the above-mentioned TMA works are based on the on-off switching function, i.e., rectangular pulses in time domain. Until recently, in order to create more degrees of freedom for manipulating the beamforming patterns in harmonic frequencies, other switching functions, such as periodic sum-of-weighted-cosine (SWC) pulses in [8], rather than the conventional rectangular pulses are investigated.

One major drawback associated with the TMA is its low power efficiency due to the switch-off of some antenna elements periodically in time domain [9]. The energy is dissipated within the beamforming networks. This, however, has recently been addressed by using reconfigurable beamforming networks [10], [11], which dynamically re-route energy to active array elements. In this paper, we focus on demonstrating the capability of TMAs for multiple access applications. Only on-off switching (rectangular pulses) and fixed switching networks are considered. The extension to other switching functions and reconfigurable beamforming networks are subject to future study.

3 TMA WITH A SINGLE RF CHAIN

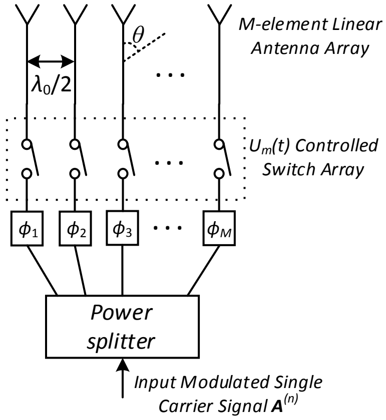

Fig. 1 Structure of time modulated linear array with a single RF chain.

In this paper, a single RF chain TMA structure shown in Fig. 1 is investigated. It consists of a linear M-element antenna array connected to a suite of single-pole single-throw switches and phase shifters (with phase delay ϕ_m). A 1-to-M power splitter with equal power splitting ratios is used to drive the entire array with modulated single RF carrier signals $\boldsymbol{A}^{(n)}$ at frequency f_0. The superscript '(n)' refers to the n^{th} input symbol in a stream and $n = 1, 2, \ldots, N$. It is assumed that array elements are $\lambda_0/2$ uniformly spaced, where λ_0 is the wavelength corresponding to the frequency f_0. The active element patterns of each element in the array are assumed to be identical and isotropic.

The far-field radiation patterns of the TMA in free space can be expressed as

$$\begin{aligned}\boldsymbol{F}(\theta) &= e^{j2\pi f_0 t}\sum_{m=0}^{M-1}\left[\boldsymbol{B}_m^{(n)} e^{-j\phi_m}\boldsymbol{U}_m(t)\, e^{j\frac{2\pi}{\lambda_0}\cdot\frac{m\lambda_0}{2}\sin\theta}\right] \\ &= e^{j2\pi f_0 t}\sum_{m=0}^{M-1}\left[\boldsymbol{B}_m^{(n)} e^{-j\phi_m}\boldsymbol{U}_m(t)\, e^{jm\pi\sin\theta}\right] \quad , \qquad (1)\end{aligned}$$

where θ is the spatial direction relative to the array boresight, seen in Fig. 1. Because the mirror symmetry exists with respect to the array, only $\theta \in [-\pi/2, \pi/2]$ is considered. $\boldsymbol{B}_m^{(n)}$ denotes the signal at the input of the phase shifter in the m^{th} array chain ($m = 1, 2, \ldots, M$), and, for ideal power splitters, it is expressed as

$$\boldsymbol{B}_m^{(n)} = \frac{1}{\sqrt{M}}\boldsymbol{A}^{(n)}. \qquad (2)$$

$\boldsymbol{U}_m(t)$ in (1) refers to the on-off function in time domain of the m^{th} switch, see illustrations in Fig. 2. ‘1’ represents ‘on’ of the switch and ‘0’ represents ‘off’. For the two cases shown in Fig. 2, $\boldsymbol{U}_m(t)$ in one repetition period T_p can be mathematically written as

$$\boldsymbol{U}_m(t) = \begin{cases} 1 & t_m^s \le t \le t_m^e \\ 0 & otherwise \end{cases} \qquad when \quad t_m^e > t_m^s, \tag{3}$$

or

$$\boldsymbol{U}_m(t) = \begin{cases} 1 & 0 \le t \le t_m^e, \ and \ t_m^s \le t \le T_p \\ 0 & otherwise \end{cases} \qquad when \quad t_m^e < t_m^s \quad . \tag{4}$$

Here, t_m^s and t_m^e refer to the switch-on and switch-off time instants respectively, seen in Fig. 2, and we define $\Delta t_m = t_m^e - t_m^s$ (when $t_m^e > t_m^s$) or $\Delta t_m = t_m^e - t_m^s + T_p$ (when $t_m^e < t_m^s$).

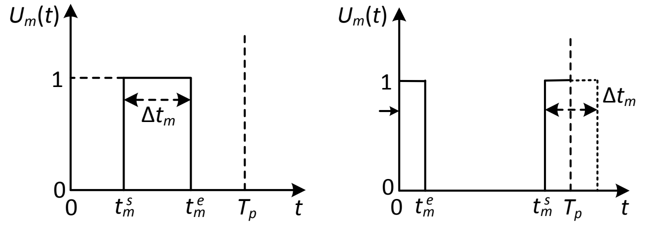

(a) (b)

Fig. 2 Illustration of on-off switch function $\boldsymbol{U}_m(t)$ in time domain.

When being expanded to Fourier series, (3) and (4), however, result in the same expression in (5).

$$\boldsymbol{U}_m(t) = \tau_m \sum_{q=-\infty}^{\infty} \mathrm{sinc}(q\tau_m) \cdot e^{j2q\pi f_p t} \cdot e^{-jq\pi(2\tau_m^s + \tau_m)} \tag{5}$$

Here $\mathrm{sinc}(x) = \sin(\pi x)/(\pi x)$, $f_p = 1/T_p$, $\tau_m = \Delta t_m / T_p$, and $\tau_m^s = t_m^s / T_p$.

Substituting (2) and (5) into (1), we get

$$\boldsymbol{F}(\theta) = \frac{\boldsymbol{A}^{(n)}}{\sqrt{M}} \sum_{q=-\infty}^{+\infty} \left(e^{j2\pi(f_0 + qf_p)t} \sum_{m=0}^{M-1} \tau_m \, \mathrm{sinc}(q\tau_m) \cdot e^{j\pi\left[m \sin\theta - \frac{\phi_m}{\pi} - q(\tau_m + 2\tau_m^s)\right]} \right). \tag{6}$$

The far-field patterns $\boldsymbol{F}(\theta)$ can be translated into the detected signals at the receiver side located along spatial direction θ.

4 PROPOSED TMA MULTIPLE ACCESS SCHEME

The purpose of multiple access is to transfer independent data to different users. We add subscript q to $\boldsymbol{F}(\theta)$ to denote the signals at frequency f_0+qf_p, thus,

$$\boldsymbol{F}_q(\theta) = \frac{\boldsymbol{A}^{(n)}}{\sqrt{M}} \sum_{m=0}^{M-1} \tau_m \, \mathrm{sinc}(q\tau_m) \cdot e^{j\pi\left[m \sin\theta - \frac{\phi_m}{\pi} - q(\tau_m + 2\tau_m^s)\right]}. \tag{7}$$

The RF carrier term $e^{j2\pi(f_0+qf_p)t}$ is deliberately suppressed, as it will be removed at receiver sides before data decoding.

It is assumed that the first user is located along θ_0, and the user detects signals at the frequency f_0, i.e., $q = 0$ in (7),

$$\boldsymbol{F}_0(\theta) = \frac{\boldsymbol{A}^{(n)}}{\sqrt{M}} \sum_{m=0}^{M-1} \tau_m \cdot e^{j\pi\left(m \sin\theta - \frac{\phi_m}{\pi}\right)}. \tag{8}$$

From (8) it can be obtained that in order to achieve beamforming along θ_0, ϕ_m has to satisfy

$$\phi_m = m\pi \sin(\theta_0), \tag{9}$$

and $\frac{1}{\sqrt{M}} \sum_{m=0}^{M-1} \tau_m$ determines the beamforming gain towards the first user. Under these settings the first user receives a scaled $\boldsymbol{A}^{(n)}$, which is the modulated symbol randomly selected from the constellation points in In-phase and Quadrature (IQ) plane. For example, when BPSK modulation is used, $\boldsymbol{A}^{(n)} \in \{1, -1\}$.

When other users are located along θ_q, and receive signals at frequencies of f_0+qf_p respectively, we get

$$\boldsymbol{F}_q(\theta_q) = \frac{\boldsymbol{A}^{(n)}}{\sqrt{M}} \sum_{m=0}^{M-1} \tau_m \, \mathrm{sinc}(q\tau_m) \cdot e^{j\pi\left[m(\sin\theta_q - \sin\theta_0) - q(\tau_m + 2\tau_m^s)\right]}. \tag{10}$$

In order for parallel data transmission to different users, $\boldsymbol{F}_q(\theta_q)$ for each q needs to be synthesised for all possible constellation points in IQ space independently. For instance, when $\boldsymbol{A}^{(n)} \in \{1, -1\}$ as the example we took earlier, if we want to transmit another BPSK data stream, modulated at frequency f_0+f_p, to receivers along θ_1, we need to find out four sets of τ_m and τ_m^s, which are able to create four possible constellation combinations $[\boldsymbol{F}_0(\theta_0), \boldsymbol{F}_1(\theta_1)]$, namely $(\boldsymbol{C}_0, \boldsymbol{C}_1)$, $(\boldsymbol{C}_0, -\boldsymbol{C}_1)$, $(-\boldsymbol{C}_0, \boldsymbol{C}_1)$ and $(-\boldsymbol{C}_0, -\boldsymbol{C}_1)$, where $\boldsymbol{C}_0 = \frac{1}{\sqrt{M}} \sum_{m=0}^{M-1} \tau_m$ and $\boldsymbol{C}_1$ can be any complex numbers that make the synthesis having solutions.

In general cases, when there are Q users, and each associated transmission has P_q constellation points, a total number of $\prod_q P_q$ sets of τ_m and τ_m^s are required to be synthesised. There are no closed-form solutions. However, they can be efficiently obtained via population-based optimisation algorithms, such as particle swarm optimisation (PSO) [12, 13]. It is noted that τ_m and $\tau_m^s \in (0, 1)$.

5 TMA MULTIPLE ACCESS EXAMPLES AND SIMULATION RESULTS

In this section, two examples are presented to validate the proposed TMA multiple access scheme, and show the detailed synthesis procedures.

5.1. Two users

The TMA synthesis, seeking appropriate sets of τ_m and τ_m^s, for a two-user scenario is described in this subsection. In this example, it is assumed that two users are positioned along $\theta_0 = 0$ (first user) and $\theta_1 = \pi/6$ (second user), and they intend to receive signals at frequencies f_0 and f_0+f_p (i.e., $q = 1$), respectively. BPSK modulation is chosen for the first user, while QPSK for the second user.

From (9), we get $\phi_m = m\pi\sin(\theta_0) = 0$. Thus, the far-field pattern at the frequency f_0 is

$$\boldsymbol{F}_0(\theta) = \frac{\boldsymbol{A}^{(n)}}{\sqrt{M}} \sum_{m=0}^{M-1} \tau_m \cdot e^{jm\pi\sin\theta}, \tag{11}$$

where $\boldsymbol{A}^{(n)} \in \{1, -1\}$ as BPSK is adopted. When replacing θ with $\theta_0 = 0$ in (11), it is noticed that the BPSK modulation format at the first receiver side is preserved as long as $\sum_{m=0}^{M-1}\tau_m$ is a constant.

When $q = 1$, i.e., at the frequency f_0+f_p, it is obtained from (10) that

$$\boldsymbol{F}_1(\theta_1) = \frac{\boldsymbol{A}^{(n)}}{\sqrt{M}} \sum_{m=0}^{M-1} \tau_m \,\mathrm{sinc}(\tau_m) \cdot e^{j\pi\left[m(\sin\theta_1)-\left(\tau_m+2\tau_m^s\right)\right]}. \tag{12}$$

As discussed in Section 4, we could use optimisation algorithms to synthesise 8 sets of τ_m and τ_m^s so that $\boldsymbol{F}_1(\theta_1)/\boldsymbol{A}^{(n)} \in \{\boldsymbol{C}_1e^{j0}, \boldsymbol{C}_1e^{j\pi/2}, \boldsymbol{C}_1e^{j\pi}, \boldsymbol{C}_1e^{-j\pi/2}\}$ for each $\boldsymbol{A}^{(n)} \in \{1, -1\}$, where $\boldsymbol{C}_1$ is a complex number determining the gain towards the second user. In the meantime, $\sum_{m=0}^{M-1}\tau_m$ needs to be kept as a constant. It is noted that the solution to the above problem is not unique.

Since in this example, there are only two users, and low-order modulation, i.e., BPSK and QPSK, is used, one solution can be directly obtained by observing structures of (11) and (12). This is elaborated as below.

- When we make $\tau_m = \tau$ for any m, $\sum_{m=0}^{M-1}\tau_m = M\tau$, and $\boldsymbol{F}_0(\theta_0) = \sqrt{M}\tau\boldsymbol{A}^{(n)}$ preserves the BPSK modulation format for the first user;
- We rewrite (12) in (13) by considering $\tau_m = \tau$. From (13), it can be observed that when τ_m^s satisfies four conditions in (14), individually, four standard QPSK constellation points in IQ space for the second user can be formed, no matter what $\boldsymbol{A}^{(n)}$ is selected. Operator 'mod(x, y)' in (14) returns the remainder after division of x by y;

$$\boldsymbol{F}_1(\theta_1) = \frac{\tau}{\sqrt{M}}\mathrm{sinc}(\tau)e^{-j\pi\tau}\boldsymbol{A}^{(n)}\sum_{m=0}^{M} e^{j\pi\left(m\sin\theta_1-2\tau_m^s\right)} \tag{13}$$

$$\begin{cases} \mathrm{mod}\left(m\sin\theta_1 - 2\tau_m^s, 2\right) = 0 \\ \mathrm{mod}\left(m\sin\theta_1 - 2\tau_m^s, 2\right) = 1/2 \\ \mathrm{mod}\left(m\sin\theta_1 - 2\tau_m^s, 2\right) = 1 \\ \mathrm{mod}\left(m\sin\theta_1 - 2\tau_m^s, 2\right) = -1/2 \end{cases} \tag{14}$$

- The beamforming gain towards the first user is $G_1(\tau) = \sqrt{M}\tau$, while the gain towards the second user is $G_2(\tau) = \sqrt{M}\tau\,\mathrm{sinc}(\tau)$ when (14) is satisfied. Fig 3 plots the $G_1(\tau)$ and $G_2(\tau)$. By choosing different τ, we can adjust the gains towards the two users.

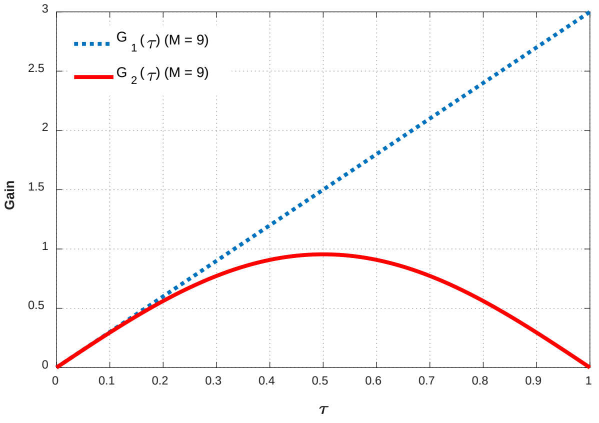

Fig. 3 Beamforming gains towards two users as a function of τ. In this example, it is assumed that $\tau_m = \tau$ and $M = 9$.

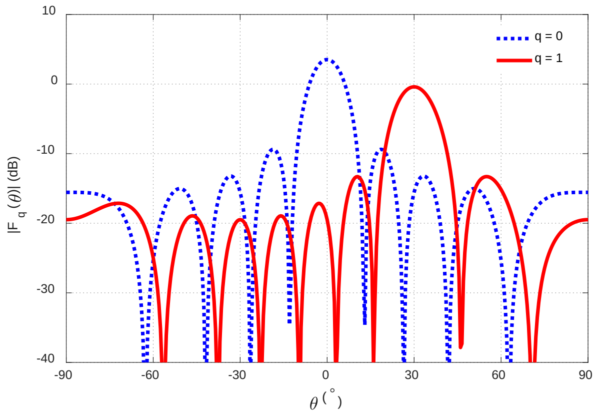

Fig. 4 Far-field radiation patterns (magnitude in dB) at two different frequencies f_0 and f_0+f_p in the synthesised two-user TMA system in Table**1**. Beamforming gains towards the two users are achieved.

The synthesis results for the 8 transmission combinations, namely, either one of two BPSK symbols for the user1 along θ_0 and either one of four QPSK symbols for the user2 along θ_1, are listed in Table **1**. In this example, it is assumed that $\theta_0 = 0$, $\theta_1 = \pi/6$, $M = 9$, and $\tau_m = \tau = 0.5$. It can be clearly observed that two independent data streams can be transmitted simultaneously to the two users by dynamically selecting, at the symbol rates, one out of the 8 sets of switch control functions $\boldsymbol{U}_m(t)$ according to the baseband data combinations. It is worth noting that different to the broadcasted multiple access schemes, e.g., traditional single RF chain TDMA, FDMA and CDMA, the beamforming gains towards the two users are obtained, see Fig. 4. The beamforming is achieved at two different frequencies, i.e., different q.

5.2 Three users

When there are more than two users that need to be served simultaneously, it can be difficult to find solutions by directly observing (10) and (11). Thus, optimisation algorithms are exploited. In this subsection, we choose PSO to synthesise a three-user 9-element ($M = 9$) TMA. The three users are assumed to be positioned along $\theta_0 = 0$, $\theta_1 = \pi/6$, and $\theta_2 = -\pi/4$, and all three independent data streams are BPSK modulated, but at three different frequencies, f_0 ($q = 0$), f_0+f_p ($q = 1$), and f_0+2f_p ($q = 2$), respectively.

The parameters used in the PSO algorithm, similar to those used in [14], are:

- Swarm particle numbers: 800;
- Iteration numbers: 3000;
- Initial inertia weight: 0.9;
- Final inertia weight: 0.4;
- Acceleration constant associated with best particle position: 2;
- Acceleration constant associated with best global position: 2;
- Boundary condition: bounce method.

Table **1**. The synthesis results for 8 transmission combinations in the two-user TMA transmitters. The first user along θ_0 is BPSK modulated and the second user along θ_0 is QPSK modulated.

Simulation parameters: $\theta_0 = 0$ (first user); $\theta_1 = \pi/6$ (second user); $M = 9$; $\tau_m = \tau = 0.5$								
m	τ_m^s	τ_m^s	τ_m^s	τ_m^s	τ_m^s	τ_m^s	τ_m^s	τ_m^s
1	0	0.75	0.50	0.25	0.50	0.25	0	0.75
2	0.25	0	0.75	0.50	0.75	0.50	0.25	0
3	0.50	0.25	0	0.75	0	0.75	0.50	0.25
4	0.75	0.50	0.25	0	0.25	0	0.75	0.50
5	0	0.75	0.50	0.25	0.50	0.25	0	0.75
6	0.25	0	0.75	0.50	0.75	0.50	0.25	0
7	0.50	0.25	0	0.75	0	0.75	0.50	0.25
8	0.75	0.50	0.25	0	0.25	0	0.75	0.50
9	0	0.75	0.5	0.25	0.5	0.25	0	0.75
	When $\boldsymbol{A}^{(n)} = 1$ $\boldsymbol{F}_0(\theta_0) = 1.5$ $\boldsymbol{F}_1(\theta_1)$ $=0.95\angle 0$	When $\boldsymbol{A}^{(n)} = 1$ $\boldsymbol{F}_0(\theta_0) = 1.5$ $\boldsymbol{F}_1(\theta_1)$ $=0.95\angle \pi/2$	When $\boldsymbol{A}^{(n)} = 1$ $\boldsymbol{F}_0(\theta_0) = 1.5$ $\boldsymbol{F}_1(\theta_1)$ $=0.95\angle \pi$	When $\boldsymbol{A}^{(n)} = 1$ $\boldsymbol{F}_0(\theta_0) = 1.5$ $\boldsymbol{F}_1(\theta_1)$ $=0.95\angle -\pi/2$	When $\boldsymbol{A}^{(n)} = -1$ $\boldsymbol{F}_0(\theta_0) = 1.5$ $\boldsymbol{F}_1(\theta_1)$ $=0.95\angle 0$	When $\boldsymbol{A}^{(n)} = -1$ $\boldsymbol{F}_0(\theta_0) = 1.5$ $\boldsymbol{F}_1(\theta_1)$ $=0.95\angle \pi/2$	When $\boldsymbol{A}^{(n)} = -1$ $\boldsymbol{F}_0(\theta_0) = 1.5$ $\boldsymbol{F}_1(\theta_1)$ $=0.95\angle \pi$	When $\boldsymbol{A}^{(n)} = -1$ $\boldsymbol{F}_0(\theta_0) = 1.5$ $\boldsymbol{F}_1(\theta_1)$ $=0.95\angle -\pi/2$
	User1:BPSK 1 User2:QPSK11	User1:BPSK 1 User2:QPSK01	User1:BPSK 1 User2:QPSK00	User1:BPSK 1 User2:QPSK10	User1:BPSK 0 User2:QPSK11	User1:BPSK 0 User2:QPSK01	User1:BPSK 0 User2:QPSK00	User1:BPSK 0 User2:QPSK10

Table **2**. The synthesis results for 8 transmission combinations in the three-user TMA transmitters. The first, second, and third users are positioned along θ_0, θ_1, and θ_2 respectively, and three independent data streams are all BPSK modulated.

Simulation parameters: $\theta_0 = 0$ (first user); $\theta_1 = \pi/6$ (second user); $\theta_2 = -\pi/4$ (third user); $M = 9$																
m	τ_m	τ_m^s	τ_m	τ_m^s	τ_m	τ_m^s	τ_m	τ_m^s	τ_m	τ_m^s	τ_m	τ_m^s	τ_m	τ_m^s	τ_m	τ_m^s
1	0.25	0.85	0.70	0.66	0.45	0.23	0.19	0.19	0.64	0.18	0.43	0.29	0.21	0.09	0.27	0.87
2	0.25	0.17	0.39	0.95	0.08	0.78	0.42	0.51	0.23	0.40	0.36	0.58	0.21	0.98	0.14	0.28
3	0.33	0.45	0.57	0.32	0.43	0.82	0.70	0.73	0.44	0.78	0.32	0.93	0.56	0.34	0.46	0.43
4	0.68	0.43	0.05	0.70	0.80	0.89	0.20	0.14	0.32	0.06	0.68	0.88	0.22	0.60	0.72	0.38
5	0.42	0.56	0.28	0.90	0.26	0.18	0.41	0.31	0.28	0.45	0.60	0.80	0.28	0.84	0.64	0.76
6	0.76	0	0.57	0.91	0.72	0.53	0.27	0.72	0.33	0.69	0.39	0.53	0.63	0.91	0.22	0
7	0.34	0.34	0.21	0.53	0.29	0.83	0.16	0.65	0.74	0.59	0.23	0.85	0.52	0.25	0.37	0.15
8	0.22	0.68	0.67	0.43	0.29	0.04	0.59	0.98	0.12	0.90	0.38	0.11	0.74	0.44	0.52	0.41
9	0.34	0.72	0.17	0.74	0.29	0.43	0.66	0.21	0.49	0.32	0.21	0.45	0.25	0.73	0.27	0.92
	When $\boldsymbol{A}^{(n)} = 1$ $\boldsymbol{F}_0(\theta_0) = 1.2$ $\boldsymbol{F}_1(\theta_1) = 0.6$ $\boldsymbol{F}_2(\theta_2) = 0.3$		When $\boldsymbol{A}^{(n)} = 1$ $\boldsymbol{F}_0(\theta_0) = 1.2$ $\boldsymbol{F}_1(\theta_1) = 0.6$ $\boldsymbol{F}_2(\theta_2) = -0.3$		When $\boldsymbol{A}^{(n)} = 1$ $\boldsymbol{F}_0(\theta_0) = 1.2$ $\boldsymbol{F}_1(\theta_1) = -0.6$ $\boldsymbol{F}_2(\theta_2) = 0.3$		When $\boldsymbol{A}^{(n)} = 1$ $\boldsymbol{F}_0(\theta_0) = 1.2$ $\boldsymbol{F}_1(\theta_1) = -0.6$ $\boldsymbol{F}_2(\theta_2) = -0.3$		When $\boldsymbol{A}^{(n)} = -1$ $\boldsymbol{F}_0(\theta_0) = -1.2$ $\boldsymbol{F}_1(\theta_1) = 0.6$ $\boldsymbol{F}_2(\theta_2) = 0.3$		When $\boldsymbol{A}^{(n)} = -1$ $\boldsymbol{F}_0(\theta_0) = -1.2$ $\boldsymbol{F}_1(\theta_1) = 0.6$ $\boldsymbol{F}_2(\theta_2) = -0.3$		When $\boldsymbol{A}^{(n)} = -1$ $\boldsymbol{F}_0(\theta_0) = -1.2$ $\boldsymbol{F}_1(\theta_1) = -0.6$ $\boldsymbol{F}_2(\theta_2) = 0.3$		When $\boldsymbol{A}^{(n)} = -1$ $\boldsymbol{F}_0(\theta_0) = -1.2$ $\boldsymbol{F}_1(\theta_1) = -0.6$ $\boldsymbol{F}_2(\theta_2) = -0.3$	
	User1:BPSK 1 User2:BPSK 1 User3:BPSK 1		User1:BPSK 1 User2:BPSK 1 User3:BPSK 0		User1:BPSK 1 User2:BPSK 0 User3:BPSK 1		User1:BPSK 1 User2:BPSK 0 User3:BPSK 0		User1:BPSK 0 User2:BPSK 1 User3:BPSK 1		User1:BPSK 0 User2:BPSK 1 User3:BPSK 0		User1:BPSK 0 User2:BPSK 0 User3:BPSK 1		User1:BPSK 0 User2:BPSK 0 User3:BPSK 0	

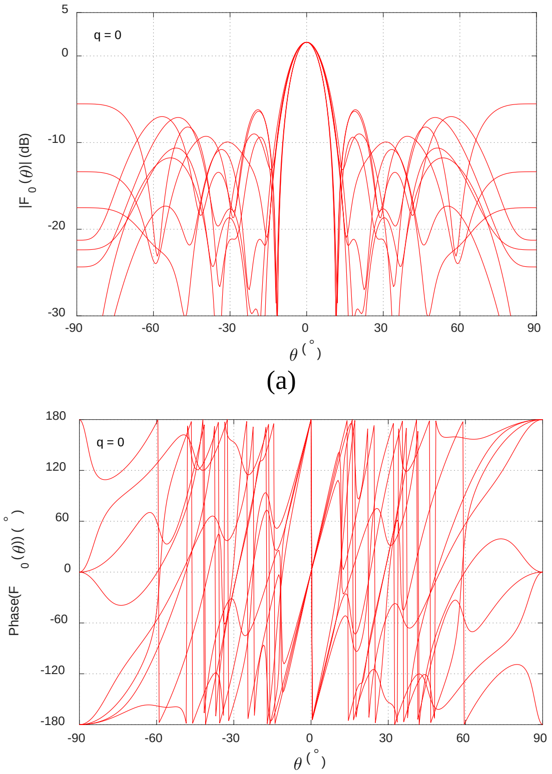

(a)

(b)

Fig. 5 Far-field radiation patterns, (a) magnitude and (b) phase, for the first user along θ_0 = 0 at frequency f_0 in the three-user TMA example shown in Table **2**.

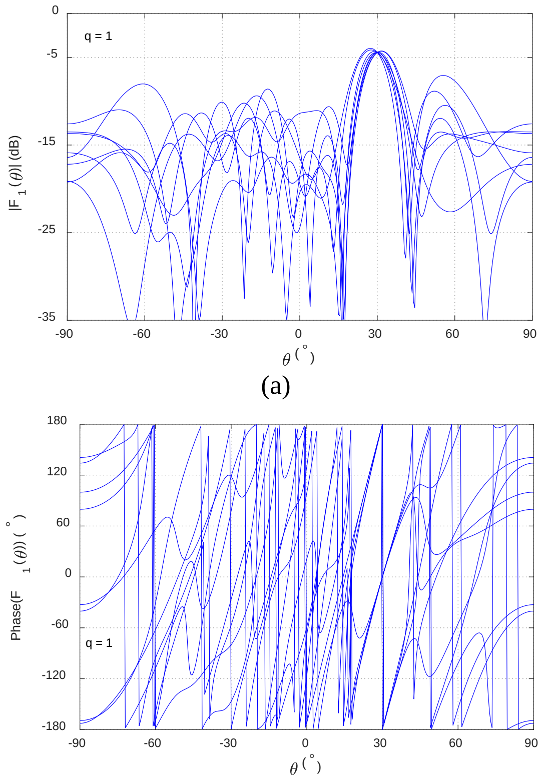

(a)

(b)

Fig. 6 Far-field radiation patterns, (a) magnitude and (b) phase, for the second user along $\theta_1 = \pi/6$ at frequency f_0+f_p in the three-user TMA example shown in Table **2**.

The synthesis results are listed in Table **2**, and the far-field radiation patterns, i.e., 8 transmission combinations for each user at their assigned frequencies, are depicted in Fig. 5 to Fig. 7, for both magnitudes and phases. It can be clearly observed that three independent BPSK modulated signals are formed at three different frequencies, i.e., different *q*, along their spatial directions, and beamforming gains are enabled.

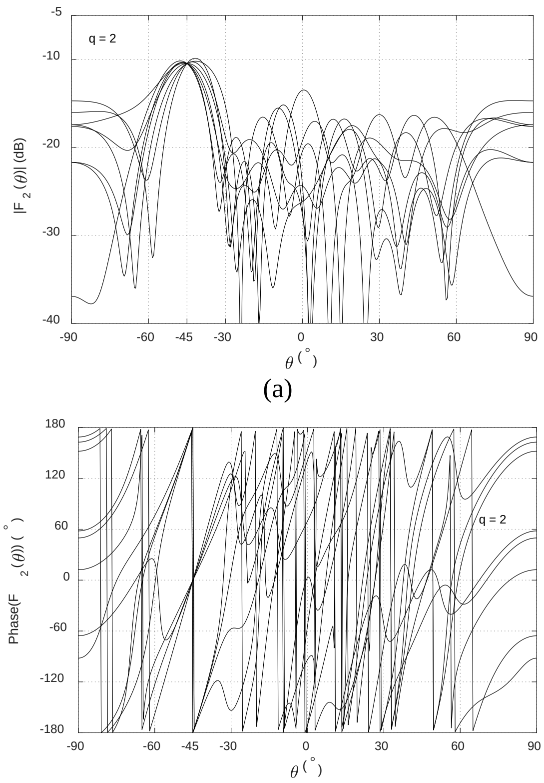

(a)

(b)

Fig. 7 Far-field radiation patterns, (a) magnitude and (b) phase, for the third user along $\theta_2 = -\pi/4$ at frequency f_0+2f_p in the three-user TMA example shown in Table **2**.

CONCLUSION

This paper presented a novel multiple access architecture by exploiting single RF chain TMAs. Compared with other multiple access schemes, it exhibits a number of advantages, such as low cost and complexity (due to a single RF chain), low PAPR and high energy efficiency (due to the frequency expansion by switches). The operation principle was elaborated, and synthesis procedures were presented and illustrated using two examples. The proposed single RF chain TMA multiple access scheme will find applications where low-cost low-energy access points for line-of-sight multi-user mobile wireless communications are preferable. This paper is by no means a complete study on this TMA multiple access architecture, and its extensions for *a*) adjustments of beamforming gains towards different users, *b*) higher modulation schemes, and *c*) multipath mobile environment are subject to further investigations.

CONFLICT OF INTEREST

No conflict of interest.

Mr. X. He's work was supported by Education Department Research Project of Shaanxi Province Government under Grant No.2013JK1131. Dr. Y. Ding's work was supported by Heriot-Watt University Academic Start-up funding. Mr. G. Huang's work was supported by PhD Oversea-exchange Scholarship from Guilin University of Electronic Technology (China).

REFERENCES

[1] S. D. Ilcev, "Space division multiple access (SDMA) applicable for mobile satellite communications," *2011 10th International Conf. Telecommun. in Modern Satellite Cable and Broadcasting Services (TELSIKS)*, Nis, 2011, pp. 693-696.

[2] W.-Q Wang, H. So and A. Farina, "An overview on time/frequency modulated array processing," *IEEE J. Sel. Topics Signal Process.*, vol. 11, no. 2, pp. 228–246, Mar. 2017.

[3] D. Ni, S. Yang and Y. Chen, "Subarrayed 4D antenna arrays with tapered amplitude excitations," *2016 IEEE International Symp. on Antennas Propag. (APSURSI)*, Fajardo, 2016, pp. 707-708.

[4] W. H. Kummer, A. T. Villeneuve, T. S. Fong and F. G. Terrio, "Ultra low sidelobes from time-modulated arrays," *IEEE Trans. Antennas Propag.*, vol. 11, no. 6, pp. 633–639, Nov. 1963.

[5] C. He, X. Liang, Z. Li, J. Geng and R. Jin, "Direction finding by time modulated array with harmonic characteristic analysis," *IEEE Antennas Wireless Propag. Lett.*, vol. 14, no. 1, pp. 642–645, 2015.

[6] J. Guo, S. Yang and Q. Zhu, "4D-arrays for MIMO radar applications," *Proceedings of 2014 3rd Asia-Pacific Conf. Antennas Propag.*, Harbin, 2014, pp. 139-142.

[7] Q. Zhu, S. Yang, R. Yao and Z. Nie, "Directional modulation based on 4-D antenna arrays," *IEEE Trans. Antennas Propag.*, vol. 62, no. 2, pp. 621-628, Feb. 2014.

[8] R. Maneiro-Catoira, J. C. Brégains, J. A. García-Naya and L. Castedo, "Enhanced time-modulated arrays for harmonic beamforming, " *IEEE J. Sel. Topics Signal Process.*, vol. 11, no. 2, pp. 259-270, Mar. 2017.

[9] Q. Zhu, S. Yang, R. Yao and Z. Nie, "Gain improvement in time-modulated linear arrays using SPDT switches," *IEEE Antennas Wireless Propag. Lett.*, vol. 11, pp. 994-997, 2012.

[10] J. Chen *et al.*, "Instantaneous gain optimization in time modulated array using reconfigurable power divide/combiner," *IEEE Antennas Wireless Propag. Lett.*, vol. 17, no. 4, pp. 530-533, Apr. 2018.

[11] J. Chen *et al.*, "Efficiency improvement of time modulated array with reconfigurable power divider/combiner," *IEEE Trans. Antennas Propag.*, vol. 65, no. 8, pp. 4027-4037, Aug. 2017.

[12] Y. Shi and R. Eberhart, "A modified particle swarm optimizer," *in Evolutionary Computation Proceedings, 1998. IEEE World Congress on Computational Intelligence, The 1998 IEEE Int. Conf.*, pp. 69-73, 1998.

[13] Y. Ding and V. Fusco, "Directional modulation transmitter synthesis using particle swarm optimization," *2013 Loughborough Antennas Propag. Conf. (LAPC)*, Loughborough, 2013, pp. 500-503.

[14] Y. Ding and V. Fusco, "BER driven synthesis for directional modulation secured wireless communication," *Int. J. Microw. Wireless Technol.*, vol. 6, no. 02, pp. 139-149, 2014.

Received: May 11, 2018 Revised: June 05, 2018 Accepted: